A Brain Extraction Algorithm for Brain Magnetic Resonance Images

Geng-Jin Liou [#1], Kuo-Hsing Huang[*2], Yue-Jing He [#3],Chen-Chung Liu[#4]

[#] *Department of Electronic Engineering, National Chin-Yi University of Technology*

No.57, Sec.2, Chung-Shan Rd., Taiping, Taichung, Taiwan

[1]tony89243@gmail.com

[3]yuejing@ncut.edu.tw

[4]ccl@ncut.edu.tw

[*] *Management Information Systems, Central Taiwan University of Science and Technology*

No.666, Buzih Rd., Beitun, Taichung, Taiwan

[2]kshuang@ctust.edu.tw

***Abstract*— The main goal of this paper is to improve region growing scheme and mathematical morphology scheme simultaneously, to present a simple algorithm to effectively extract brain from a brain magnetic resonance (MR) image. The presented brain extraction algorithm is a hybrid method, it combines active contours (or deformable models) approach, mathematical morphology, and statistic regression to extract brain from a brain MR image effectively and accurately. For evaluating the performance of the presented algorithm on real MR data, the brain MR datasets provided by the Alzheimer's Disease Neuroimaging Initiative (ADNI) are used. The experimental results show that the brain extracted by the presented algorithm approximately follows the gold-standard of ANDI.**

***Keywords*—Magnetic resonance (MR), brain, extract, active contour, regression.**

1. INTRODUCTION

Magnetic resonance (MR) imaging is a medical diagnostic technology developed in the past 30 years [1], [2]. The hydrogen nuclei of water molecules in human body are paramagnetism. The magnetic resonance shall be appeared when these water molecules are located in a gradient magnetic field. MR imagingI transforms these magnetic resonance signals into a spatial magnetic resonance image[3], [4]. Due to MR imaging has noninvasive properties and can provide very high resolution images for living tissues, MR imaging can be used to detect the states of cell, tissue and organ[5],[6]. It also can be applied to distinguish the difference between the tumor and the cancer cells, and to find the distribution of brain cells [3], [7]. At present, MR imaging is widely used to diagnose and monitor the activity of brain disease such as brain stroke, cerebellar atrophy, multiple sclerosis, Parkinson’s disease, Alzheimer’s disease and so on [5]-[9].

Corrective measuring of brain volume is an important issue in brain clinical medicine and basic research. In the pathology field, to measure the variations in brain volume can provide the basis data for brain diagnosis. If one can measure the gray matter (GM) and white matter (WM) volumes simultaneously, then he can really help some special diagnosis of brain disease, such as Alzheimer's disease [7]-[10]. MR imaging offers different pulse sequences and different contrast parameters to yield multiple sets of body images, to present the variety characteristics of different brain tissues [11], [12]. So, the brain MR images are very suitable for brain tissue segmentation and the corresponding volume measure. On the other hand, we can utilize image processing technologies to strengthen the lesions or the characteristics of some brain tissues to enhance the identification rate of brain tissues. Nowadays, brain MR imaging has become an important focus in current brain quantitative morphological research [13]-[15].

In brain MR imaging, for corrective measuring of brain volume and for performing good quantitative studies, various tissues in a MR imaging head scan has to be defined specifically. Previously, manual brain tissue segmentation was frequently performed by skilled experts [15]-[17]. Manual segmentation by expert radiologists is reliable, but it is extremely tedious, labor intensity, time-consuming and susceptible to substantial intra-rater and inter-rater variability [15]-[18]. Moreover, a large number of brain MR images are taken by the brain screening program and these brain MR images are manually segmented by experts to detect the signs of abnormalities. The necessity of reading a huge number of brain MR images causes high false positive, and also causes high false negative in which disease lesions are missed due to fatigue or distraction of radiologists [16], [17]. So, an accurate automatic brain MR image segmentation system is required, it can save numerous manpower and let radiologists take more time on the suspected lesions to achieve early diagnosis and effective monitoring of real brain diseases.

Many of these automatic brain MR image segmentation systems need the extraction of the whole brain from the head MR image, either because the whole brain is checked such as in Alzhiemer’s studies [17], [18] or because automatic brain tissue extraction becomes easier and more accurate if the skull and scalp have been removed [19]. Brain extraction is the process of segmenting brain from non-brain tissues such as skull, scalp, eyes, or neck in whole-head MR images and without removing any part of the brain. A wide variety of techniques for automatic brain extraction have been proposed over the past decade. The most popular brain extraction methods are region growing methods [2], [8], [11], [12] and mathematical morphology methods [15], [16], [18], [19]. Region growing methods emerge neighbor pixels of source seed pixel to form an area by predefined criteria [12]. The drawback of Region growing method is that user has to select the source seeds and threshold values [2]. The mathematical morphology methods extract the brain through a series of thresholding and morphological operations, for instance, using morphological opening and eroding to distinct the brain tissues from the surrounding non-brain tissues and utilizing morphological dilating and closing to fill up the holes inside the brain tissues. The disadvantage of mathematical morphology methods is that they have to first binarize the original image into object and background regions [16].

The main goal of this paper is to improve region growing scheme and mathematical morphology scheme simultaneously, to present a simple algorithm to effectively extract brain from a MR head image. The presented brain extraction algorithm is a hybrid method, it combines active contours (or deformable models) approach, mathematical morphology, and statistic regression to extract brain from a MR head image effectively and accurately. The remainder of this paper is organized as follows: The presented brain extraction algorithm is illustrated in Section 2. Experiment results are presented in Section 3. Finally, we conclude this paper in Section 4.

2. PROPOSED BRAIN EXTRACTION ALGORITHM

In order to construct an accurate brain extraction algorithm for brain MR images, several schemes are used in this paper. The overall brain extraction algorithm for brain MR images is shown in FIGURE 1.There are mainly three stages involved in the algorithm: (i) head region segmented by using Sobel edge detector, (ii) source and sink seeds found by histogram analysis and least squares fitting of Rayleigh function, (iii) final brain extraction by random walk scheme. The details of these stages used in the presented brain extraction algorithm are described in the following subsections.

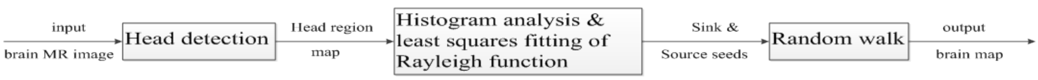

Fig. 1. Flowchart of the presented brain extraction algorithm for brain MR images.

2.1. Head Region Segmentation

Since to extract the brain in a region of interesting (ROI), head region, is more effective than that in the whole brain MR image. In the proposed computer aided detection system of brain lesions, we apply median filter to filter out noises and smooth the input brain MR image, utilize the Sobel edge detector and the most outmost edge detecting scheme to extract the head region from the noise-deleted and smoothed brain MR image.

2.1.1. Median filtering [20]

The median filter is a nonlinear spatial filter, is a powerful tool at removing outlier type noise. It does suit for the job at preserving edges of an image. The filter mask simply defines what pixels must be included in the median calculation. The computation of the median filter starts at ordering those n pixels defined by the filter mask, in the order from minimum to maximum value of the pixels as given in Equ. (3).

$$F_0 \leq F_1 \leq F_2 \cdots \leq F_{n-2} \leq F_{n-1} \qquad (1)$$

where F_0 denotes the minimum and F_{n-1} is the maximum of all the pixels in the filter calculation. The output of the median filter is the median of these values and is given by

$$F_{med} = \begin{cases} \dfrac{F_{n/2} + F_{n/2-1}}{2} & for \quad n \quad even \\ F_{n/2} & for \quad n \quad odd \end{cases} \qquad (2)$$

Typically, an odd number of filter elements are chosen, to avoid the additional step in averaging the middle two pixels of the order set when the number of elements is even.

The input brain MR image may be interfered by noise. So, it needed a filter to reduce noise and get rid of misjudgment in image recognition. The median filter has the suitable filter property that we need, so, we take it as a processor in brain extraction system to reduce the noise and increase the extraction rate.

2.1.2. Head contour detection

The Sobel gradient mask is one of popular edge detection methods [20]. Figure 2 shows the Sobel gradient mask; Figure 2(a) is a mask type, Figure 2(b) and Figure 2(c) are the values of masks that are used for detecting the horizontal and vertical edge, respectively. In head contour detection stage, we first apply the Sobel gradient mask on the noise-deleted and smoothed brain MR image to detect all edges in the image. Then we detect and combine the uppermost edge, the lowest edge, the leftmost edge, and the rightmost edge to form the head contour. The inside region of the head contour is taken as the extracted head region.

Z1	Z2	Z3
Z4	Z5	Z6
Z7	Z8	Z9

(a)

-1	-2	-1
0	0	0
1	2	1

(b)

-1	0	1
-2	0	2
-1	0	1

(c)

Fig. 2. The Sobel gradient mask, (a) the mask pixels, (b) $f_x(x, y)$, (c) $f_y(x, y)$.

2.2. Histogram Analysis and Seeds Selection

The main tissue types in a head region are gray matter (GM), white matter (WM), Cerebrospinal fluid (CSF), skull, and eyes. Where, the brain region (GM, WM) and non-brain region (skull, eyes) are separated by CSF (a dark ring). On the other hand, these regions GM, WM, CSF, skull, and eyes appear in distinct intensity levels in the histogram of a head region. The histogram usually has three peaks; they are located in dark region composed by CSF, in gray region composed by GM and skull, and in bright region composed by WM and eyes, respectively. The histogram shapes around each peak are almost the same as the horizontal-shifted Rayleigh probability density function in probability theory and statistic, respectively. After the histogram analysis and the analysis of tissue geometric locations, we find that the source seeds have to be GM and exclude skull from the gray peak region, and the sink seeds have selected from CSF.

To select source seeds, the mathematic morphology erosion operator with structure element disk with radius equals 0.02 co-axis length of head region is employed to erode the head region to retain part of GM and delete other tissues firstly. Then, a least squares fitting of a horizontal-shifted Rayleigh curve is performed on the gray peak region of the historgram of the eroded head map to find the mean, μ, and the standard deviation, σ, for the best fit horizontal-shifted Rayleigh function. In the eroded head map, the pixels with pixel value located in the interval, [μ-0.002σ, μ+0.002σ], are selected as the source seeds. Different radius concentric rings with width 5 pixels are taken as detectors to select sink seeds.

2.3. Brain Extraction by Random Walk Scheme

For image segmentation, random walk scheme is a semi-automated interactive algorithm proposed by Grady [21]. The main steps are: The original image is first presented with its corresponding weighted graph G= (V, W), in which each pixel is the vertex V, and W is the weight between the neighbor vertices. The weight is defined by the Gaussian weight function:

$$w(\upsilon_i,\upsilon_j) = \exp(-\beta(g(\upsilon_i) - g(\upsilon_j))^2), \qquad (5)$$

where $g(\upsilon_i)$ is the intensity of the pixel υ_i and β is a free parameter.

For the weighted graph, all vertices are divided into a marked vertices set V_M , and an unmarked vertices set V_U , such that $V_M \cup V_U = V$ and $V_M \cap V_U = \phi$. Finally, due to the probability problem for a random walk is the same as a Dirichlet problem, and Dirichlet problem can be evaluate from the graph Laplacian matrix defined as the follows.

$$L(i,j) = \begin{cases} \sum_{\upsilon_i} w(\upsilon_i,\upsilon_j), & \upsilon_i = \upsilon_j \\ w(\upsilon_i,\upsilon_j), & \upsilon_i \ and\ \upsilon_j\ are\ adjacent\ vertices. \\ 0, & otherwise \end{cases} \qquad (3)$$

So the image segmentation with random walk is transformed to the Dirichlet problem and the image segmentation results are obtained by solving the corresponding Dirichlet problem. In this paper, the random walk scheme using source seeds selected from GM and sink seeds selected from CSF is conducted on the head region map to extract brain from brain MR images.

3. EXPERIMENTAL RESULTS

Based on the spin-lattice relaxation time (Tl), the local variations of spin-spin relaxation time (T2), and proton density (PD), MR imaging systems can create many images with different characteristics in the same body section [5],[13]. The MR image types are T1-weighted (T1w), T2-weighted (T2w), and PD-weighted (PD).Three type brain MR images are shown in Figure 3. Since T1w MR images offer outstanding contrast for the different brain tissues. Moreover, the brain region extracted from T1w images can be mapped to other type MR images. We first apply the presented algorithm on T1w MR images, and then map the result to T2w and PD images. In order to evaluate the performance of the presented brain extraction algorithm, it is applied on simulated MR images offered by the Alzheimer's Disease Neuroimaging Initiative (ADNI) database (http://www.loni.ucla.edu/ADNI). Figure 4 shows a brain extraction example utilized the presented algorithm.

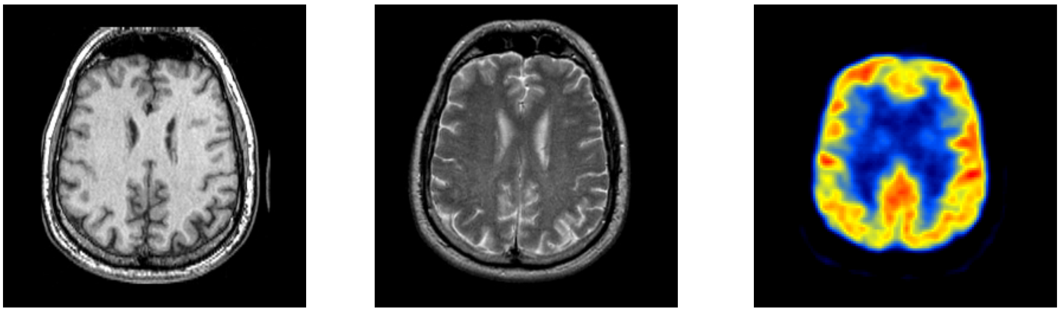

(a) (b) (c)

Fig. 3. MR image types (a) T1-weighted (b) T2-weighted (c) PD.

The brain extraction results are analyzed according the normalized performance metrics to show the different performance features of the extraction algorithms. These normalized performance metrics are misclassification error (*ME*) function, relative foreground area error (*RFAE*), accuracy (*Acc*), and extraction error rate (*EER*) [22]. *ME*, *RFAE*, *Acc*, and *EER* are varying from 0 for a perfectly correct segmentation to 1 for a completely error case. These performance measures are illustrated as the follows:

(i) The misclassification error (*ME*) evaluates the inaccuracy of an algorithm which is defined as:

$$ME = 1 - \frac{TP + TN}{TP + FN + TN + FP} = \frac{FN + FP}{TP + FN + TN + FP}, \quad (4)$$

where *TP*, *TN*, *FP* and *FN* represent the areas of true positive, true negative, false positive and false negative, respectively.

(ii) The relative foreground area error (RFAE) evaluates the region mismatch between the extracted object and the ground- truth object and is defined as:

$$RFAE = \begin{cases} \dfrac{(TP+FN)-(FP+TP)}{TP+FN} = \dfrac{FN-FP}{TP+FN} & if\ (FP+TP) < (TP+FN) \\ \dfrac{(FP+FN)-(TP+FN)}{FP+TP} = \dfrac{FP-FN}{FP+TP} & if\ (FP+TP) \geq (TP+FN) \end{cases}. \quad (5)$$

(iii) The accuracy evaluates the closeness of the extracted object to the ground- truth object and is defined as:

$$Accuracy = (TP+TN)/(TP+TN+FN+FP), \quad (6)$$

(iv) The extraction error rate (*EER*) evaluates the failure rate of the algorithm. It is the summation of under- extraction rate (*UER*) and the over- extraction (*OER*) rate and is defined as:

$$EER = UER + OER = \frac{FN}{TP+FN} + \frac{FP}{TP+FN}. \quad (7)$$

These normalized performance metrics of the presented algorithm applied on ADNI database are listed in Table 1. These experimental results show that the proposed algorithm is an effective and precise scheme for brain extracting from brain MR images.

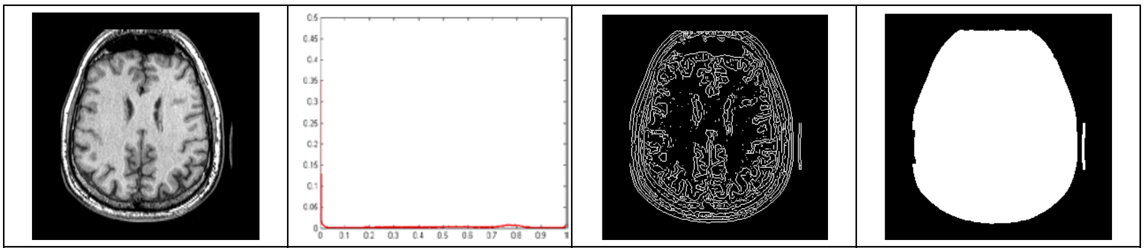

(a) (b) (c) (d)

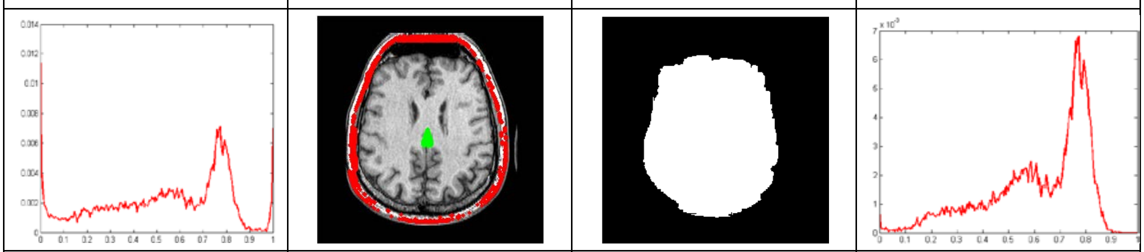

(e) (f) (g) (h)

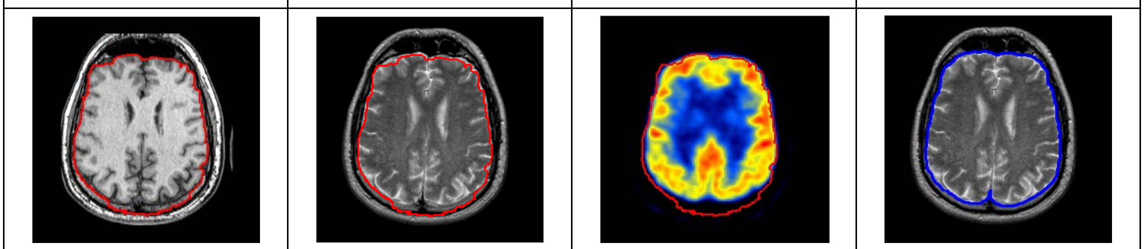

(i) (j) (k) (l)

Fig. 4. A brain extraction example utilized the presented algorithm: (a) original T1-weighted brain MR image, (b) histogram of the original T1-weighted brain MR image, (c) after Sobel edge detecting, (d) extracted head region, (e) histogram of the extracted head region, (f) selected source and sink seeds, (g) extracted brain by random walk, (h) histogram of the extracted brain, (i) extracted brain on T1-weighted MR image, (j) extracted brain on T2-weighted MR image , (k) extracted brain on PD MR image, (l) the gold-standard.

TABLE 1

THE NORMALIZED PERFORMANCE METRICS OF THE PRESENTED ALGORITHM APPLIED ON ADNI DATABASE

Item	***FN***	***TN***	***TP***	***FP***	***ME2***	***RFAE***	***ACC***	***EER***
Value	1338	10658	21266	748	0.0383	0.0261	0.9387	0.0923

4. CONCLUSIONS

Almost all the automatic brain MR image segmentation systems need the extraction of the whole brain from the brain MR image, either because the whole brain is checked such as in Alzhiemer’s studies or because automatic brain tissue extraction becomes easier and more accurate if the skull and scalp have been removed. The presented brain extraction algorithm is a hybrid method, it combines active contours (or deformable models) approach, mathematical morphology, and statistic regression to extract brain from a brain MR image effectively and accurately. For evaluating the performance of the presented algorithm on real MR data, the brain MR datasets provided by the Alzheimer's Disease Neuroimaging Initiative (ADNI) are used. The experimental results show that the brain extracted by the presented algorithm approximately follows the gold-standard of ANDI.

ACKNOWLEDGMENT

This research was supported by the National Science Council R.O.C. under Grant NSC 101-2221-E-167-038.

REFERENCES

[1] H. H. Zhuang, D. J. Valentino, and A. W. Toga, “Skull-stripping magnetic resonance images using a model-based level set,” *NeuroImage*, vol. 32, pp. 79 – 82, 2006.

[2] J.G. Park and C. Lee, “Skull Stripping Based On Region Growing For Magnetic Resonance Brain Images”, *NeuroImage*, vol. 47, pp. 1394-1407, 2009.

[3] L. Lemieux, G. Hagemann, K. Krakow, and F.G. Woermann, “Fast, accurate and reproducible automatic segmentation of the brain in T1-weighted volume MRI data,” *Magnetic resonance in Medicine*,

vol. 42, no.1, pp. 127-135, 1999.

[4] D.W. Shattuck, S.R. Sandor-Leahy, K.A. Schaper, D.A. Rottenberg, and R.M. Leahy, “Magnetic resonance image tissue classification using a partial volume model,” *NeuroImage*, vol. 13, pp. 856-876, 2001.

[5] F. Se´gonne, A.M. Dale, E. Busa, M. Glessner, D. Salat, H.K. Hahn, B. Fischl, A hybrid approach to the skull stripping problem in MRI, *NeuroImage*, vol. 22, pp.1060– 1075, 2004.

[6] M.S. Smith, “Fast Robust Automated Brain Extraction,” *Human Brain Mapping*, vol. 17, pp. 143-155, 2002.

[7] M.S. Atkins and B.T. Mackiewich, “Fully Automatic Segmentation of the Brain in MRI”, *IEEE Transactions Medical Imaging*, vol. 17(1), pp. 98-107, 1998.

[8] J. S. Suri, “Two-dimensional fast magnetic resonance brain segmentation,” *IEEE Trans. Med. Biol.*, pp. 84 – 95, 2001.

[9] S. A. Sadananthan, W. Zheng, M. W.L. Chee, V. Zagorodnov, Skull stripping using graph cuts, *NeuroImage*, vol. 49, pp. 225–239, 2010.

[10] C. Baillard, P. Hellier, and C. Barillot, “Segmentation of brain 3D MR images using level sets and dense registration,” *Med. Image Anal.*, vol. 5, pp. 185 – 194, 2001

[11] A.F. Goldszal, C. Davatzikos, D.L. Pham, M.X.H. Yan, R.N. Bryan and S.M. Resnick, “An Image Processing System for Qualitative and Quantitative Volumetric Analysis of Brain Images”, *Journal Comput. Assist. Tomogr.*, vol. 22, no. 5, pp. 827-837, 1998.

[12] R. Roslan, N. Jamil, R. Mahmud, Skull Stripping Magnetic Resonance Images Brain Images: Region Growing versus Mathematical Morphology, *International Journal of Computer Information Systems and Industrial Management Applications*, vol. 3, pp.150-158, 2011.

[13] T. Kapur, W. E. L. Grimson, W.M. Wells and R. Kikinis, “Segmentation of Brain Tissue from Magnetic Resonance Images”, *Medical Image Analysis*, vol. 1, no. 2, pp. 109-127, 1996.

[14] K. K. Leung, J. Barnes, M. Modat, G. R. Ridgway, J.W. Bartlett, N.C. Fox, S. Ourselin, ADNI: Brain MAPS: An automated, accurate and robust brain extraction technique using a template library. *NeuroImage*, vol. 55, pp. 1091–1108, 2011.

[15] R, Roslan, N. Jamil and R. Mahmud, “Skull Stripping of MRI Brain Images using Mathematical Morphology”, *IEEE-EBMS Conference on Biomedical Engineering and Sciences (IECBES 2010)*, 2010.

[16] D.W. Shattuck, S.R. Sandor-Leahy, K.A. Schaper, D.A. Rottenberg, and R.M. Leahy, “Magnetic resonance image tissue classification using a partial volume model,” *NeuroImage*, vol. 13, pp. 856-876, 2001.

[17] J. Gao and M. Xie, “Skull-stripping MR Brain Images using Anisotropic Diffusion Filtering and Morphological Processing”, *IEEE International*

Symposium on Computer Network and Multimedia Technology, pp. 1-4, 2009.

[18] A. H. Zhuang, D. J. Valentino, A. W. Toga, Skull-stripping magnetic resonance brain images using a model-based level set, *NeuroImage*, vol. 32, pp.79 – 92, 2006.

[19] S. F. Eskildsen, P. Coupé, V. Fonova, J. V. Manjón, K. K. Leung, N. Guizard, S. N. Wassef, L. R. Østergaard, D. L. Collins, BEaST: Brain Extraction based on nonlocal Segmentation Technique, *NeuroImage,* vol. 59, no. 3, pp. 2362-2373, 2012.

[20] Sheng-Wen Zheng, Yung-Tsang Chang, Chen-Chung Liu, A Breast Tumors Segmentation Scheme for Digital Mammograms, *The 2nd Conference on Applications of Innovation & Invention,* pp.678- 685, 2012.

[21] Jheng-Jhe Tsai, Chun-Yuan Yu, Chen-Chung Liu, Shyr-Shen Yu, A Novel Exudate Detection Scheme on Retinal Images, *The 2nd Conference on Applications of Innovation & Invention,* pp.665- 671, 2012.

[22] Chen-Chung Liu, Chung-Yen Tsai, Jui Liu, Chun-Yuan Yu, Shyr-Shen Yu, “A pectoral muscle segmentation algorithm for digital mammograms using Otsu thresholding and multiple regression analysis,” *Computers & Mathematics with Applications*, vol. 64, pp.1100-1107, 2012.